Mechanism and Machine Theory 87 (2015) 57–69

Contents lists available at ScienceDirect

Mechanism and Machine Theory

journal homepage: www.elsevier.com/locate/mechmt

Modeling analysis and experimental study for the friction of a ball screw

Nannan Xu [a,*], Wencheng Tang [a], Yongjiang Chen [a], Dafei Bao [a], Yujie Guo [b]

[a] Department of Mechanical Engineering, Southeast University, Nanjing 211189, China
[b] Aerospace Structures and Computational Mechanics, Delft University of Technology, Delft 2629 HS, The Netherlands

ARTICLE INFO

Article history:
Received 20 March 2014
Received in revised form 7 November 2014
Accepted 30 December 2014
Available online 17 January 2015

Keywords:
Ball screw
Friction
Creep analysis
Friction distribution
Slipping item of Heathcote

ABSTRACT

This paper aims to develop a new systematic creep analysis model to calculate the friction of a ball screw. In order to investigate the friction behavior better, a proper transformed coordinate system was established. Through the creep analysis and the principle of force balance, the creep parameters can be easily obtained, such as the vertical creep ratio, the horizontal creep ratio and the spin ratio acting on three contact areas. Based on roll contact theory, the ball screw friction can be predicted more accurately. The effectiveness of the creep analysis model is verified through experiments. Furthermore, the influence of the creep parameters on the ball screw friction and friction distribution will be discussed. The study not only provides a new perspective and approach for the study of ball screw friction, but also provides the theory basis for reasonably reducing the friction and improving the mechanical efficiency of a ball screw.

1. Introduction

Due to the relatively low cost and insensitivity to inertia variation and external forces, the application of ball screws in the positioning machine tool has been promoted further especially in the aspects of high speed and precision. This has led to increasing attention being paid to the influence of ball screw friction on precision and mechanical efficiency [1]. After considerable research, it has been gradually realized that the influence of the friction element on the dynamic performance of ball screws cannot be ignored especially under the condition of high precision and speed [2].

The friction of ball screw is defined as movement resistance caused by all kinds of friction factors in a ball screw, which lead to a reduction of the mechanical efficiency of the ball screw with a loss of energy and positioning accuracy with the thermal deformation. The friction model should be quicker and more efficient to predict the energy loss and temperature rise rates. Due to similarity, there is certain inheritance between the analysis of ball screws and ball bearings, and research into ball bearings can be taken as a reference point when researching ball screws. The kinematics and dynamics analyses of ball screws should be investigated first. Jones [3] introduced the raceway control theory in the process of studying dynamics on ball bearings. In Harris's paper [4], it was demonstrated that the raceway control theory is generally valid for high-speed ball bearings and the friction behavior between a ball and the inner raceway of ball bearings was analyzed. Harris believed that the friction is generated by pressure on the ball's surface and deemed this friction behavior would lead to abrasion of the ball bearing. Based on Harris's research, Lin and Wei et al. [5] proposed a systematic theoretical method to investigate the kinematics of a ball screw using Frenet–Serret coordinates, in which the Coulomb model is used to analyze the friction between the ball and screw (or the nut). Aiming at increasing the accuracy, Olaru D et al. [6], suggested

* Corresponding author. Tel.: +86 25 52090508.
E-mail address: nnxu@seu.edu.cn (N. Xu).

http://dx.doi.org/10.1016/j.mechmachtheory.2014.12.019
0094-114X/

an improved Coulomb friction model. Based on Kamalzadeh A's [7] research, Su [8] found that the improved Coulomb friction model proposed in [6] still cannot predict the ideal result for a high-precision ball screw.

Numerous studies indicated that most of the calculations of ball screw friction were based on Coulomb friction model assuming that all balls were equally loaded and the friction between balls were ignored. In general, these methods can well meet the requirements of engineering practice under low and medium precision conditions, which have a certain application market. However, there are certain limitations to the Coulomb friction model in non-planar situations, which mean that the Coulomb model cannot essentially be used to improve the precision of ball screw friction calculations. Considering the influence of gyroscopic effect on quasi statics balance of ball bearing, Kalker [9–12] did a series of kinematics analysis on ball bearings with unlubricated contact. The model Kalker produced is not perfect enough, but it does provide an effective solution to the existing problem of ball the screw.

In order to improve the accuracy of ball screw friction calculations and to solve the above problems, the roll contact theory is used in this paper to analyze ball screw friction. The friction between the balls in the ball screw is taken in consideration and the problem of stress inequality in every circle of a ball screw is discussed. This paper is organized as follows. The homogeneous coordinate transformation systems and the ball screw friction calculated using the creep analysis model is given in Section 2. The results of the friction torque calculated by creep analysis model and the experimental measurements are compared and discussed in Section 3. The influence of the creep parameters on the friction distribution on the slipping area is also presented in Section 3. Finally, we summarize the main findings of this work and draw conclusions in Section 4.

2. Theoretical analysis

In order to calculate the friction of a ball screw, three coordinate systems are established first: global coordinate system, Frenet–Serret coordinate system and contact coordinate system. The global coordinate system, (x, y, z), is fixed at the center of the nut chassis, the screw axis is in the same direction with z axis. The Frenet–Serret coordinate system [13], (t, n, b), is fixed at the ball center whose moving trajectory is in line with the t axis direction. The contact coordinate system, $(e_\lambda, f_\lambda, g_\lambda)$, is fixed at the contact points between the ball and raceway and the contact point pointing to the ball center is coincident with the g_λ axis direction. Here, $\lambda = A$ represents the contact point between the ball and nut raceway, and $\lambda = B$ represents the contact point between the ball and screw raceway. The relationship of contact coordinate system with Frenet–Serret coordinate system and global coordinate system is shown in Fig. 1.

As shown in Fig. 1, the angle between b-axis and z-axis is α, which has the same value of helix angle. The angular velocity of screw and nut are defined as ω and ω_N, respectively. β_B and β_A represent the contact angle of the ball with respect to the screw and nut, respectively. r_b is the radius of ball.

2.1. Homogeneous coordinate transformations

In order to facilitate the systematic study of the theoretical model, the transformation relationships between the different coordinate systems must be established. The homogeneous coordinate transformations between the two coordinates (t, n, b) and (x, y, z) can be obtained through three transformations. One, the origin of the global coordinate system is translated to the intersection point H along the helix line, which is marked as $Trans(r_m \cos\theta, r_m \sin\theta, r_m\theta \tan\alpha)$. Two, the global coordinate system is rotated around the z axis by $(\theta + \pi/2)$-degree to make x and y axes coincident with t' and n' axes which are the projections of t and n axes on the $x - y$ plane, and is marked as $Rot(z, \theta + \pi/2)$, as shown in Fig. 2(a). Three, the global coordinate system is rotated around y axis by $(2\pi - \alpha)$-degree, which is marked as $Rot(y, 2\pi - \alpha)$, as shown in Fig. 2(b).

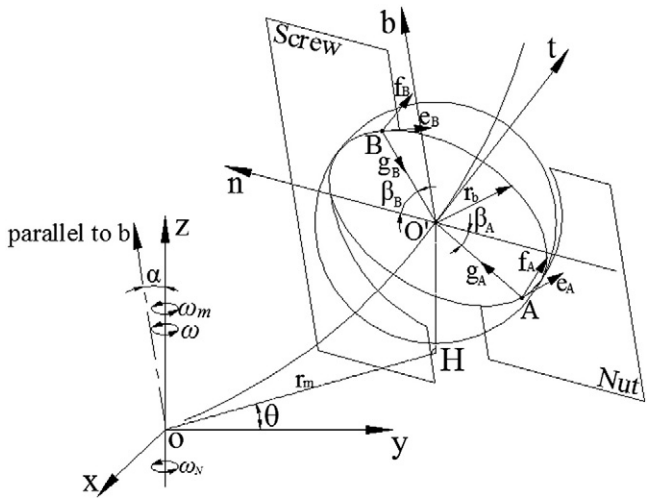

Fig. 1. Three coordinate systems.

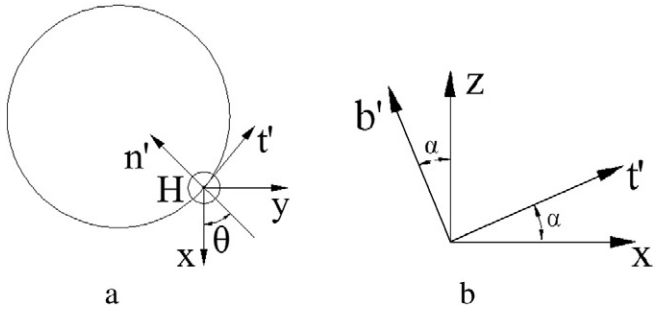

Fig. 2. Coordinate transformation.

According to the homogeneous coordinate transformation, the relation between two coordinates (t, n, b) and (x, y, z) is given as:

$$\begin{bmatrix} x \\ y \\ z \\ 1 \end{bmatrix} = Trans(r_m\cos\theta, r_m\theta\tan\alpha)Rot(z,\theta+\pi/2)Rot(y,2\pi-\alpha)$$

$$= \begin{bmatrix} 1 & 0 & 0 & r_m\cos\theta \\ 0 & 1 & 0 & r_m\sin\theta \\ 0 & 0 & 1 & r_m\theta\tan\alpha \\ 0 & 0 & 0 & 1 \end{bmatrix} \begin{bmatrix} \cos\theta(+\pi/2) & -\sin\theta(+\pi/2) & 0 & 0 \\ \sin\theta(+\pi/2) & \cos\theta(+\pi/2) & 0 & 0 \\ 0 & 0 & 1 & 0 \\ 0 & 0 & 0 & 1 \end{bmatrix} \begin{bmatrix} \cos2(\pi-\alpha) & 0 & \sin2(\pi-\alpha) & 0 \\ 0 & 1 & 0 & 0 \\ -\sin2(\pi-\alpha) & 0 & \cos2(\pi-\alpha) & 0 \\ 0 & 0 & 0 & 1 \end{bmatrix}$$

$$= \begin{bmatrix} -\cos\alpha\sin\theta & -\cos\theta & \sin\alpha\sin\theta & r_m\cos\theta \\ \cos\alpha\cos\theta & -\sin\theta & -\sin\alpha\cos\theta & r_m\sin\theta \\ \sin\alpha & 0 & \cos\alpha & \frac{\theta L}{2\pi} \\ 0 & 0 & 0 & 1 \end{bmatrix} \times \begin{bmatrix} t \\ n \\ b \\ 1 \end{bmatrix} \tag{1}$$

where the L is the length of the screw's pitch.

Similarly, the homogeneous coordinate transformations between $(e_\lambda, f_\lambda, g_\lambda)$ and (t, n, b) can be stated as:

$$\begin{bmatrix} t \\ n \\ b \\ 1 \end{bmatrix} = \begin{bmatrix} 0 & 1 & 0 & 0 \\ -\sin\beta_B & 0 & \cos\beta_B & r_b\cos\beta_B \\ \cos\beta_B & 0 & \sin\beta_B & r_b\sin\beta_B \\ 0 & 0 & 0 & 1 \end{bmatrix} \times \begin{bmatrix} e_B \\ f_B \\ g_B \\ 1 \end{bmatrix} \tag{2a}$$

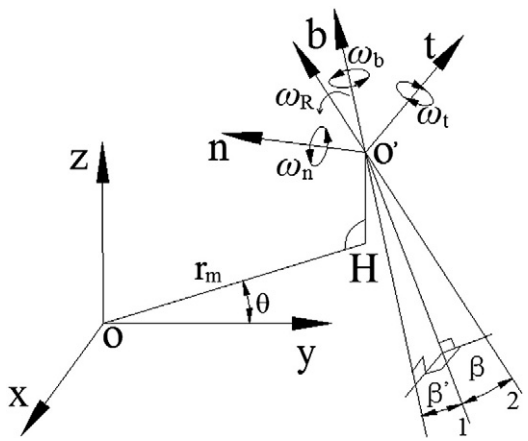

Fig. 3. The position of third coordinate system.

and

$$\begin{bmatrix} t \\ n \\ b \\ 1 \end{bmatrix} = \begin{bmatrix} 0 & 1 & 0 & 0 \\ \sin\beta_A & 0 & \cos\beta_A & r_b\cos\beta_A \\ \cos\beta_A & 0 & -\sin\beta_A & -r_b\sin\beta_A \\ 0 & 0 & 0 & 1 \end{bmatrix} \times \begin{bmatrix} e_A \\ f_A \\ g_A \\ 1 \end{bmatrix}. \tag{2b}$$

2.2. Creep analysis

Prior to making a creep analysis of ball screw, it is necessary to solve the spin angular velocity. The model of spin motion is shown in Fig. 3. The 2-axis is coincident with the spinning axis of the ball. The projection of the 2-axis in the $t-b$ plane is defined as 1-axis. The angle between 1-axis and 2-axis is β, and the angle between 1-axis and b-axis is β'. The spin angular velocity and pitch radius of the ball screw are defined as ω_R and r_m, respectively.

As shown in Fig. 3, ω_t, ω_n, ω_b are given as follows:

$$\omega_t = \omega_R\cos\beta\sin\beta' \tag{3a}$$

$$\omega_b = \omega_R\cos\beta\cos\beta' \tag{3b}$$

$$\omega_n = \omega_R\sin\beta. \tag{3c}$$

2.2.1. Creep analysis between the ball and nut

As shown in Fig. 1, three axial components of the nut angular velocity (ω_N) in the e_A- , f_A- , and g_A-directions can be written as:

$$V_{Ne} = -\omega_N[r_m + (r_b - \delta_N)\cos\beta_A] \tag{4a}$$

$$V_{Nf} = 0 \tag{4b}$$

$$\omega_{Ng} = -\omega_N\sin\beta_A \tag{4c}$$

where δ_N is the normal elastic deformation between the ball and nut, which can be calculated based on Hertz contact theory.

In the same way, three axial components of the ball's spin angular velocity (ω_R) in the e_A- , f_A- , and g_A-directions can be stated as:

$$V_{bNe} = -(r_b - \delta_N)(\omega_n\cos\beta_A + \omega_b\sin\beta_A) \tag{5a}$$

$$V_{bNf} = \omega_t(r_b - \delta_N) \tag{5b}$$

$$\omega_{bNg} = \omega_b\cos\beta_A - \omega_n\sin\beta_A. \tag{5c}$$

According to the roll contact theory [12], rolling velocity between the ball and nut is given as:

$$|V_{rA}| = \sqrt{(V_{bNe} + V_{Ne})^2 + \left(V_{bNf} + V_{Nf}\right)^2}\Big/2 \tag{6}$$

There are $|V_{Nf}| << |V_{Ne}|$ and $|V_{bNf}| << |V_{bNe}|$ under the normal working state of ball screw condition. Rolling velocity between the ball and nut can be simplified as:

$$V_{rA} \approx -(V_{bNe} + V_{Ne})/2 = [\omega_N r_m + (r_b - \delta_N)(\omega_n\cos\beta_A + \omega_b\sin\beta_A + \omega_N\cos\beta_A)]/2. \tag{7}$$

Substituting Eqs. (3a)–(3c) into Eqs. (4a)–(4c) and Eqs. (5a)–(5c), the vertical creep ratio (ξ_{eA}), horizontal creep ratio (ξ_{fA}) and spin ratio (φ_A) are obtained based on the roll contact theory as:

$$\xi_{eA}=\frac{V_{bNe}-V_{Ne}}{V_{rA}}=2\frac{\omega_N r_m-(r_b-\delta_N)(\omega_R\cos\beta\cos\beta'\cos\beta_A+\omega_R\sin\beta\sin\beta_A-\omega_N\cos\beta_A)}{\omega_N r_m+(r_b-\delta_N)(\omega_R\cos\beta\cos\beta'\cos\beta_A+\omega_R\sin\beta\sin\beta_A+\omega_N\cos\beta_A)} \tag{8a}$$

$$\xi_{fA}=\frac{V_{bNf}-V_{Nf}}{V_{rA}}=2\frac{(r_b-\delta_N)\omega_R\cos\beta\sin\beta'}{\omega_N r_m+(r_b-\delta_N)(\omega_R\cos\beta\cos\beta'\cos\beta_A+\omega_R\sin\beta\sin\beta_A+\omega_N\cos\beta_A)} \tag{8b}$$

$$\varphi_A=\frac{\omega_{bNg}-\omega_{Ng}}{V_{rA}}=2\frac{\omega_R\sin\beta\cos\beta_A-\omega_R\cos\beta\cos\beta'\sin\beta_A+\omega_N\sin\beta_A}{\omega_N r_m+(r_b-\delta_N)(\omega_R\cos\beta\cos\beta'\cos\beta_A+\omega_R\sin\beta\sin\beta_A+\omega_N\cos\beta_A)}. \tag{8c}$$

Considering the differential slipping caused by surface warpage of nut raceway, two components of slipping velocity in the e_A- and f_A- directions [12] can be expressed as follows:

$$C_{eA}=\xi_{eA}-f_A\varphi_A-\xi_h(f_A) \tag{9a}$$

$$C_{fA}=\xi_{fA}+e_A\varphi_A. \tag{9b}$$

$\xi_h(f_A)$ is the slipping item of Heathcote. Based on the roll contact theory, this can be calculated as follows:

$$\xi_h(f_A)=\left(1-\frac{\omega_N\cos\beta_A}{\omega_R\cos\beta\cos\beta'\cos\beta_A+\omega_R\sin\beta\sin\beta_A}\right)\frac{{f_A}^2}{2{r_b}^2}. \tag{10}$$

2.2.2. Creep analysis between the ball and screw

As shown in Fig. 1, three axial components of the screw angular velocity (ω) in the e_B- , f_B- , and g_B-directions can be obtained in the following forms:

$$V_{Se}=-\omega[r_m-(r_b-\delta_S)\cos\beta_B] \tag{11a}$$

$$V_{Sf}=0 \tag{11b}$$

$$\omega_{Sg}=-\omega\sin\beta_B \tag{11c}$$

δ_S is the normal elastic deformation between the ball and screw, which can be calculated based on Hertz contact theory.
Similarly, three axial components of the ball's spin angular velocity (ω_R) in the e_B- , f_B- , and g_B-directions can be stated as:

$$V_{bSe}=-(r_b-\delta_S)(\omega_n\cos\beta_B+\omega_b\sin\beta_B) \tag{12a}$$

$$V_{bSf}=-\omega_t(r_b-\delta_S) \tag{12b}$$

$$\omega_{bSg}=\omega_b\sin\beta_B-\omega_n\cos\beta_B. \tag{12c}$$

There are $|V_{Sf}|<<|V_{Se}|$ and $|V_{bSf}|<<|V_{bSe}|$ under the normal working condition. According to the roll contact theory and Eq. (6), rolling velocity between the ball and screw can be simplified as:

$$V_{rB}=\sqrt{(V_{bSe}+V_{Se})^2+\left(V_{bSf}+V_{Sf}\right)^2}\Big/2\approx-(V_{bSe}+V_{Se})/2=[\omega r_m+(r_b-\delta_S)(\omega_n\cos\beta_B+\omega_b\sin\beta_B-\omega\cos\beta_B)]/2 \tag{13}$$

Substituting Eqs. (3a)–(3c) into Eqs. (11a)–(11c) and Eqs. (12a)–(12c), the vertical creep ratio (ξ_{eB}), horizontal creep ratio (ξ_{fB}) and spin ratio (φ_B) can be written as:

$$\xi_{eB}=\frac{V_{bSe}-V_{Se}}{V_{rB}}=2\frac{\omega r_m-(r_b-\delta_S)(\omega_R\cos\beta\cos\beta'\cos\beta_B+\omega_R\sin\beta\sin\beta_B+\omega\cos\beta_B)}{\omega r_m+(r_b-\delta_S)(\omega_R\cos\beta\cos\beta'\cos\beta_B+\omega_R\sin\beta\sin\beta_B-\omega\cos\beta_B)} \tag{14a}$$

$$\xi_{fB}=\frac{V_{bSf}-V_{Sf}}{V_{rB}}=2\frac{-(r_b-\delta_S)\omega_R\cos\beta\sin\beta'}{\omega r_m+(r_b-\delta_S)(\omega_R\cos\beta\cos\beta'\cos\beta_B+\omega_R\sin\beta\sin\beta_B-\omega\cos\beta_B)} \tag{14b}$$

$$\varphi_B=\frac{\omega_{bSg}-\omega_{Sg}}{V_{rB}}=2\frac{\omega_R\cos\beta\cos\beta'\sin\beta_B-\omega_R\sin\beta\cos\beta_B+\omega\sin\beta_B}{\omega r_m+(r_b-\delta_S)(\omega_R\cos\beta\cos\beta'\cos\beta_B+\omega_R\sin\beta\sin\beta_B-\omega\cos\beta_B)}. \tag{14c}$$

Considering the differential slipping caused by surface warpage of screw raceway, the components of slipping velocity in the e_B- and f_B-directions [12] can be stated as:

$$C_{eB}=\xi_{eB}-f_B\varphi_B-\xi_h(f_B) \tag{15a}$$

$$C_{fB}=\xi_{fB}+e_B\varphi_B. \tag{15b}$$

$\xi_h(f_B)$ is the slipping item of Heathcote, which can be obtained as:

$$\xi_h(f_B)=\left(1+\frac{\omega\cos\beta_B}{\omega_R\cos\beta\cos\beta'\cos\beta_B+\omega_R\sin\beta\sin\beta_B}\right)\frac{{f_B}^2}{2{r_b}^2}. \tag{16}$$

2.2.3. Creep analysis between the balls

The roll contact model between balls is shown in Fig. 4. The contact coordinate system between the balls (e_m, f_m, g_m) is fixed at the contact point. The tangential direction at the contact point and f_m axis form a space angle (α). The angle between the line $o_1'm$ (or $o_2'm$) and t_1-axis(or t_2-axis) is also α which has the same value of helix angle.

As shown in Fig. 4, the three axial components of the spin angular velocity of the ball 1 (ω_{R1}) in the e_m- , f_m- , and g_m-directions can be stated as:

$$V_{me1}=(r_b-\delta_m)(\omega_{n1}\cos\alpha+\omega_{b1}\sin\alpha) \tag{17a}$$

$$V_{mf1}=\omega_{t1}(r_b-\delta_m) \tag{17b}$$

$$\omega_{mg1}=\omega_{b1}\cos\alpha-\omega_{n1}\sin\alpha. \tag{17c}$$

δ_m is the normal elastic deformation between the balls, which can be calculated based on Hertz contact theory.

In the same way, three axial components of the ball's spin angular velocity (ω_R) in the e_m- , f_m- , and g_m-directions can be expressed as:

$$V_{me2}=-(r_b-\delta_m)(\omega_{n2}\cos\alpha+\omega_{b2}\sin\alpha) \tag{18a}$$

$$V_{mf2}=-\omega_{t2}(r_b-\delta_m) \tag{18b}$$

$$\omega_{mg2}=\omega_{n2}\sin\alpha-\omega_{b2}\cos\alpha \tag{18c}$$

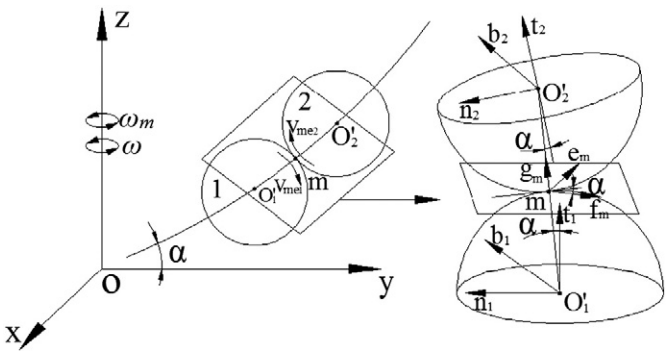

Fig. 4. Roll contact model between the balls.

where ω_{R1} and ω_{R2} can be obtained based on ω_R using homogeneous coordinate transformations (Eq.(1)). The relationship between ω_{t1}, ω_{n1} and ω_{b1} (or ω_{t2}, ω_{n2} and ω_{b2}) and ω_{R1} (or ω_{R2}) is shown in Fig. 3 and Eqs.(3a)–(3c).

There are $|V_{mf1}| << |V_{me1}|$ and $|V_{mf2}| << |V_{me2}|$ under normal working conditions for a ball screw. According to the roll contact theory and Eq. (6), rolling velocity between the balls can be simplified as:

$$\begin{aligned} V_{rm} &= \sqrt{(V_{me2}+V_{me1})^2+\left(V_{mf2}+V_{mf1}\right)}\Big/2 \approx -(V_{me1}+V_{me2})/2 \\ &= [(r_b-\delta_m)(\omega_{n2}\cos\alpha+\omega_{b2}\sin\alpha)-(r_b-\delta_m)(\omega_{n1}\cos\alpha+\omega_{b1}\sin\alpha)]/2. \end{aligned} \tag{19}$$

The vertical creep ratio (ξ_{em}), horizontal creep ratio (ξ_{fm}) and spin ratio (φ_m) can be written as:

$$\xi_{em}\frac{V_{me1}-V_{me2}}{V_{rm}} = 2\frac{(r_b-\delta_m)(\omega_{n1}\cos\alpha+\omega_{b1}\sin\alpha)+(r_b-\delta_m)(\omega_{n2}\cos\alpha+\omega_{b2}\sin\alpha)}{(r_b-\delta_m)(\omega_{n2}\cos\alpha+\omega_{b2}\sin\alpha)-(r_b-\delta_m)(\omega_{n1}\cos\alpha+\omega_{b1}\sin\alpha)} \tag{20a}$$

$$\xi_{fm} = \frac{V_{mf1}-V_{mf2}}{V_{rm}} = 2\frac{(\omega_{t1}+\omega_{t2})(r_b-\delta_m)}{(r_b-\delta_m)(\omega_{n2}\cos\alpha+\omega_{b2}\sin\alpha)-(r_b-\delta_m)(\omega_{n1}\cos\alpha+\omega_{b1}\sin\alpha)} \tag{20b}$$

$$\varphi_m = \frac{\omega_{mg1}-\omega_{mg2}}{V_{rm}} = 2\frac{\cos\alpha(\omega_{b1}+\omega_{b2})-\sin\alpha(\omega_{n1}+\omega_{n2})}{(r_b-\delta_m)(\omega_{n2}\cos\alpha+\omega_{b2}\sin\alpha)-(r_b-\delta_m)(\omega_{n1}\cos\alpha+\omega_{b1}\sin\alpha)}. \tag{20c}$$

Considering the differential slipping caused by ball surface warpage, two components of slipping velocity in the e_m- and f_m-directions [12] are given as:

$$C_{em} = \xi_{em}-f_m\varphi_m-\xi_h(f_m) \tag{21a}$$

$$C_{fm} = \xi_{fm}+e_m\varphi_m. \tag{21b}$$

$\xi_h(f_m)$ is the slipping item of Heathcote, which is expressed based on the roll contact theory and can be obtained as:

$$\xi_h(f_m) = \left(1+\frac{\omega_{n2}\sin\alpha-\omega_{b2}\cos\alpha}{\omega_{b1}\cos\alpha-\omega_{n1}\sin\alpha}\right)\frac{{f_m}^2}{2{r_b}^2} \tag{22}$$

2.3. Friction calculation of a ball

Based on Kalker's [11] theory of linear creep, vertical friction ($F_{e\lambda}$) and horizontal friction ($F_{f\lambda}$) at the contact area can be defined as:

$$F_{e\lambda} = -G{c_0}^2C_1(\xi_{e\lambda}-\xi_{h\lambda}) \tag{23a}$$

$$F_{f\lambda} = -G{c_0}^2\left(C_2\xi_{f\lambda}+C_3c_0\varphi_\lambda\right) \tag{23b}$$

where $\lambda = A, B$ and m represent different contact areas; G is the shear modulus; $c_0 = \sqrt{ab}$; a and b are semi-major axis and minor semi-axis of contact ellipse, respectively, which can be calculated based on Hertz contact theory; C_1, C_2 and C_3 are the creep coefficients [11], which can be calculated using the empirical formula as $C_1 = 0.891(a_\lambda/b_\lambda) + 3.189$, $C_2 = 1.29(a_\lambda/b_\lambda) + 2.372$ and $C_3 = 1.1091(a_\lambda/b_\lambda) + 0.379$, respectively.

It has been proven to be effective to use linear creep theory to calculate the friction under the condition of small creep and spin ratios. However, the friction error will become bigger when the creep ratio and spin ratio increase in the contact area. When the increase in creep ratio and spin ratio reaches the state of full slipping, this state can meet the conditions for applying Coulomb friction model. In order to take full advantage of the linear creep theory [12] and Coulomb friction model, the improved friction expression is stated as:

$$F_\lambda = \begin{cases} f_\lambda Q_\lambda\left[\dfrac{F_{r\lambda}}{f_\lambda Q_\lambda}-\dfrac{1}{3}\left(\dfrac{F_{r\lambda}}{f_\lambda Q_\lambda}\right)^2+\dfrac{1}{27}\left(\dfrac{F_{r\lambda}}{f_\lambda Q_\lambda}\right)^3\right] (F_{r\lambda}\le 3f_\lambda Q_\lambda) \\ f_\lambda Q_\lambda (F_{r\lambda}>3f_\lambda Q_\lambda) \end{cases} \tag{24}$$

where $\lambda = A, B$ and m represent the different contact areas; F_λ is the improved friction at contact area; f_λ is friction coefficient; $F_{r\lambda}$ represents the friction at contact area calculated by linear creep theory with $F_{r\lambda} = \sqrt{{F_{e\lambda}}^2+{F_{f\lambda}}^2}$.

2.4. Friction calculation for a ball screw

In the previous sections, the method to calculate a ball friction is introduced, in this section, a method for calculating ball screw friction will be presented. According to the three coordinate systems shown in Fig. 1, Eqs. (1) and (2b), the total friction of all balls in a circle of ball screw between the ball and nut in the global coordinate system can be given as:

$$F_A{}' = \sum_{i=1}^{n} \begin{bmatrix} -\cos\alpha\sin\theta_i & -\cos\theta_i & \sin\alpha\sin\theta_i & r_m\cos\theta_i \\ \cos\alpha\cos\theta_i & -\sin\theta_i & -\sin\alpha\cos\theta_i & r_m\sin\theta_i \\ \sin\alpha & 0 & \cos\alpha & \dfrac{\theta_i L}{2\pi} \\ 0 & 0 & 0 & 1 \end{bmatrix} \times \begin{bmatrix} 0 & 1 & 0 & 0 \\ \sin\beta_A & 0 & \cos\beta_A & r_b\cos\beta_A \\ \cos\beta_A & 0 & -\sin\beta_A & -r_b\sin\beta_A \\ 0 & 0 & 0 & 1 \end{bmatrix} \begin{bmatrix} F_{eA}{}' \\ F_{fA}{}' \\ F_{gA}{}' \\ 1 \end{bmatrix} \tag{25a}$$

where n is the number of balls in a circle of ball screw; θ_i is the position angle of different ball in a circle of ball screw; $F_{eA}{}'$, $F_{fA}{}'$ and $F_{gA}{}'$ represent the projection of the improved friction (F_A) in the e_A- , f_A- , and g_A-directions, respectively.

Similarly, the total friction between all the balls and the screw in a circle of ball screw is stated as:

$$F_B{}' = \sum_{i=1}^{n} \begin{bmatrix} -\cos\alpha\sin\theta_i & -\cos\theta_i & \sin\alpha\sin\theta_i & r_m\cos\theta_i \\ \cos\alpha\cos\theta_i & -\sin\theta_i & -\sin\alpha\cos\theta_i & r_m\sin\theta_i \\ \sin\alpha & 0 & \cos\alpha & \dfrac{\theta_i L}{2\pi} \\ 0 & 0 & 0 & 1 \end{bmatrix} \times \begin{bmatrix} 0 & 1 & 0 & 0 \\ -\sin\beta_B & 0 & \cos\beta_B & r_b\cos\beta_B \\ \cos\beta_B & 0 & \sin\beta_B & r_b\sin\beta_B \\ 0 & 0 & 0 & 1 \end{bmatrix} \begin{bmatrix} F_{eB}{}' \\ F_{fB}{}' \\ F_{gB}{}' \\ 1 \end{bmatrix} \tag{25b}$$

where $F_{eB}{}'$, $F_{fB}{}'$ and $F_{gB}{}'$ are the projection of improved friction (F_B) in the e_B- , f_B- , and g_B-directions, respectively.

Analogously, the total friction of all balls in a circle of ball screw between the balls in the global coordinate system can be expressed as:

$$F_m{}' = \sum_{i=1}^{n} \begin{bmatrix} -\cos\alpha\sin\theta_i & -\cos\theta_i & \sin\alpha\sin\theta_i & r_m\cos\theta_i \\ \cos\alpha\cos\theta_i & -\sin\theta_i & -\sin\alpha\cos\theta_i & r_m\sin\theta_i \\ \sin\alpha & 0 & \cos\alpha & \dfrac{\theta_i L}{2\pi} \\ 0 & 0 & 0 & 1 \end{bmatrix} \times \begin{bmatrix} 0 & 1 & 0 & 0 \\ \sin\alpha & 0 & \cos\alpha & r_b\cos\alpha \\ \cos\alpha & 0 & -\sin\alpha & -r_b\sin\alpha \\ 0 & 0 & 0 & 1 \end{bmatrix} \begin{bmatrix} F_{em}{}' \\ F_{fm}{}' \\ F_{gm}{}' \\ 1 \end{bmatrix} \tag{25c}$$

where $F_{em}{}'$, $F_{fm}{}'$ and $F_{gm}{}'$ represent the projection of improved friction (F_m) in the e_m- , f_m- , and g_m-directions, respectively.

Due to the inequality of balls stress distribution in the different circles of a ball screw, and processing experience accumulated at the Nanjing Technology Company [14], the following empirical expression of ball screw friction is adopted:

$$F'' = \sum_{j=1}^{p} \left(\frac{2}{3}\right)^{j-1} \left(F_A{}' + F_B{}' + F_m{}'\right) \tag{26}$$

where F'' is the ball screw friction and p is the number of the ball screw circles.

3. Results and discussion

In order to verify the new systematic creep analysis model, a ball screw of type DKFZD4012 produced by the Nanjing Technology Company is selected as the experimental ball screw. The geometric and material parameters and the operating conditions of ball screw are shown in Table 1. The friction of ball screw is difficult to measure directly in the experiment, therefore, the friction torque

Table 1
Specifications of the ball screw.

Parameters	Value	Units
I. Geometric and material parameters		
Screw pitch diameter d_m	40	*mm*
Helical pitch L	12	*mm*
Ball diameter D_w	5.953	*mm*
Raceway curvature ratio f_S, f_N	0.52	
Total number of balls Z	152	
Circles of each nut n	4	
Poisson's ratio u	0.3	
Young's modulus E	210	GPa
Friction coefficient f_λ	0.03	
II. Operating conditions		
Screw rotational speed ω	100	r/min
Preload F_p	2000	N
Axial load Fa	0	N

of ball screw is adopted. The approach is to compare the friction torque between theoretical analysis and experimental measurement to verify the friction model of ball screw. The friction torque (M) of ball screw based on the systematic creep analysis model can be obtained as:

$$M = \sum_{j=1}^{p} \left(\frac{2}{3}\right)^{j-1} [F_A{}'(r_b - \delta_N) + F_B{}'(r_b - \delta_S) + F_m{}'(r_b - \delta_m)]. \tag{27}$$

The influence of creep parameters on the friction and friction distribution on the contact area will be discussed later.

3.1. Experimental verification

The test of friction torque was carried out on a ball screw test machine. The schematic diagram of the test machine is shown in Fig. 5. One end of the ball screw is connected with the servo motor and the other end is fixed at the tailstock center. The circumferential movement of the nut is constrained by the measurement device and connecting rod. Owing to the circumferential movement limit, the nut can only drive the measurement device with axial movement along the slide guide when the ball screw is driven. The friction of the circumferential movement measured by the pressure sensor multiplied by the arm of force is the friction torque of the ball screw.

Before the start of the experiment, the ball screw ran for 5 min to make it fully lubricated. Then, the friction of the nut was measured at $\omega = 100$ r/min with no axial load, in which total 10 samples were obtained with each sample being repeated three times. In the experiment, the sampling frequency and the length of force arm were set to be 100 and 85 mm, respectively. Due to the volatility of data during measurement, both the maximum and minimum values are recorded. The friction torque test bench of ball screw is shown in Fig. 6. The experimental values of friction torque under different preload are shown in Fig. 7.

Comparisons of the friction torque obtained from the experiments and the theoretical analysis under different preloads are shown in Fig. 8. From Fig. 8 it can be seen that the theoretical and experimental values agree very well, and the friction torque increases as the ball screw preload increases, which demonstrates the effectiveness of the proposed creep analysis model. It can be observed that the theoretical prediction appears to be nonlinear when compared to the experimental measurements. This is due to the fact that, there is a nonlinear relation between the ball screw friction and the four creep parameters in the theoretical model. However, the averaged curve of experiments seems to be linear, which could be considered to be fortuitous because there may be various trends if different samples are chosen. Besides the inevitable measuring error, the factors of lubrication in ball screw and raceway waviness which may influence the friction torque are not considered in the theoretical model, and these factors may also lead to the difference between the theoretical value and experimental value. In addition, the friction coefficient derived from the recommended value in the theoretical model may also have a certain influence on the calculation results.

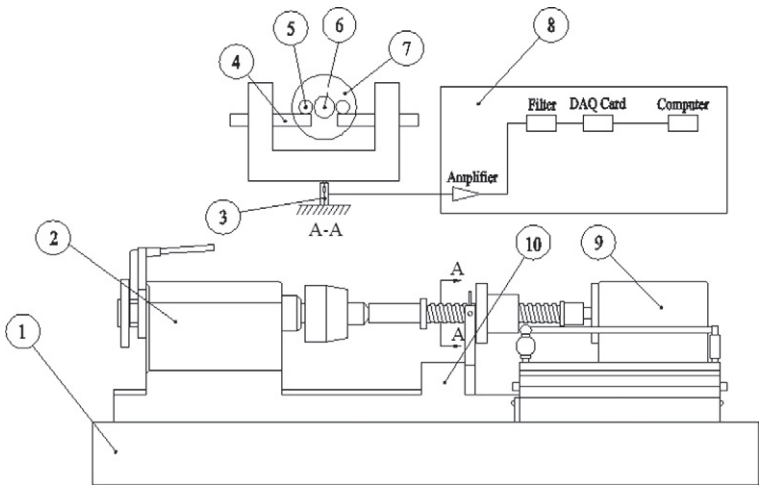

1. Experiment table; 2. Tailstock; 3. Pressure sensor; 4. Cantilever; 5. Connecting rod;

6. Screw; 7. Nut; 8. Digital data acquisition system; 9. Servo motor; 10. Measurement device

Fig. 5. Schematic diagram of ball screw performance tester: 1. Experiment table; 2. Tailstock; 3. Pressure sensor; 4. Cantilever; 5. Connecting rod; 6. Screw; 7. Nut; 8. Digital data acquisition system; 9. Servo motor; and 10. Measurement device.

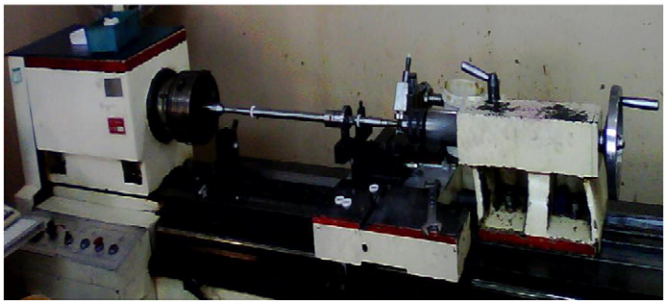

Fig. 6. The friction torque test bench of ball screw.

3.2. The influence of creep parameters on ball screw friction

According to the above theoretical analysis, it can be seen that the four creep parameters, including the vertical creep ratio, horizontal creep ratio, spin ratio and the slipping item of Heathcote, are essential factors determining the ball screw friction. Hence, the influence of each parameter on the friction needs to be discussed in detail.

The creep analysis of the different contact areas is fundamentally the same, thus a contact area is chosen to study the influence of creep parameters on the friction of ball screw. It is assumed that the other three parameters are equal to zero when studying the influence of one creep parameter on the friction of ball screw. The influences of creep parameters on the ball screw friction between the ball and nut are shown in Fig. 9. From Fig. 9, it can be seen that the ball screw friction shows a nonlinear relationship with the change of the creep ratio, including the vertical and horizontal creep ratios, without considering the spin ratio and the slipping item of Heathcote condition. This phenomenon is due to the conversion from the whole gelling state to the local micro slip and partial slip in the area between the ball and nut. Although the creep ratio and the slipping item of Heathcote are zero, the spin ratio still creates friction perpendicular to the rolling direction, which is very similar to the Magnus Effect in fluid mechanics and aerodynamics. With the increase of slipping item of Heathcote, the influence of the slipping item of Heathcote on the ball screw friction will become more obvious, and it cannot be ignored when the friction is calculated on the warpage surface.

3.3. The influence of creep parameters on friction distribution in the slipping area

Because of the elastic property of the ball and raceway in a ball screw, the little tiny elastic slip will take place on the contact areas between the ball and raceway, which means that each contact area includes two parts: the gelling area and slipping area. From Section 1, it can be seen that the previous published ball screw friction model is based on the Coulomb friction model, which results in considering either the gelling or slipping state in the area rather than both in the same time. While, using roll contact theory, the

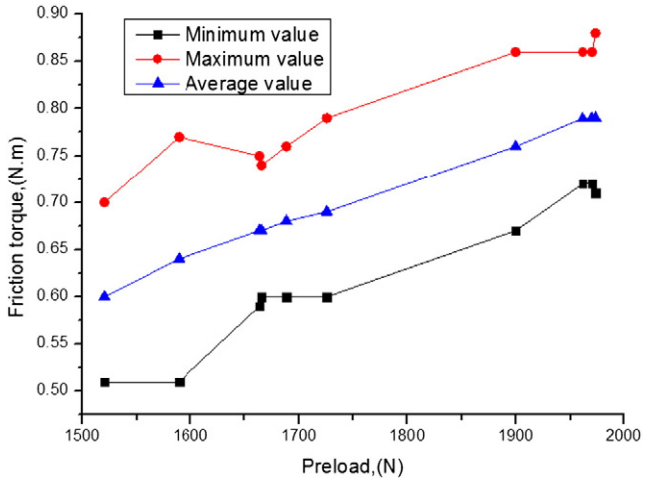

Fig. 7. The experimental measurement values.

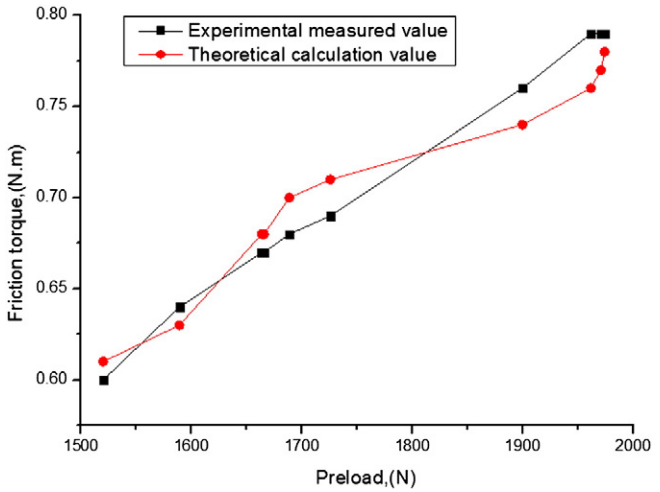

Fig. 8. The contrast between theoretical calculation value and experimental measured value.

friction and its distribution at arbitrary positions of contact area can be calculated accurately. Meanwhile the linear creep theory has been proved to be accurate for solving the contact problem in the wheel rail and ball bearing analysis, which is the main reason why the creep analysis model is used to calculate ball screw friction.

In this part, a brief analysis of the friction distribution in the slipping area between the ball and nut is presented, which provides an easy and intuitive way to understand the influence of creep parameters on ball screw friction. The ellipticity of the contact area is set to be one. Fig. 10 shows the influence of creep parameters on the friction distribution in the slipping area between the ball and nut, where the arrows denote the direction and distribution of the friction and the blank area means gelling state. The influence of one creep parameter on the friction distribution is studied based on the assumption that the other three parameters are equal to zero. Taking the vertical creep ratio (ξ_{eA}) of creep parameters for example, the influence of the vertical creep ratio ($\xi_{eA} = 0.1$) on the friction distribution is studied based on the assumption that the other three parameters, horizontal creep ratio (ξ_{fA}), spin ratio (φ_A) and slipping item of Heathcote $\xi_h(f_A)$ are equal to zero. Similarly, the influence of $\xi_{eA} = 0.3$ and $\xi_{eA} = 0.5$ on the friction distribution can be obtained. The influence of the other three parameters, horizontal creep ratio (ξ_{fA}), spin ratio (φ_A) and slipping item of Heathcote $\xi_h(f_A)$ on the friction distribution of the contact area is analyzed in the same way. It is shown in Fig. 10, the slipping friction is mainly distributed in the back edge of the contact area in the initial position. And the friction spreads from the back edge to the front edge along the contact area with the increase of ξ_{eA}, ξ_{fA} and φ_A. The friction directions are different due to different creep parameters. Whereas, it is noteworthy that the friction mainly distributes in the top and bottom edges of the contact area produced by the slipping item of Heathcote, as shown in Fig. 10.

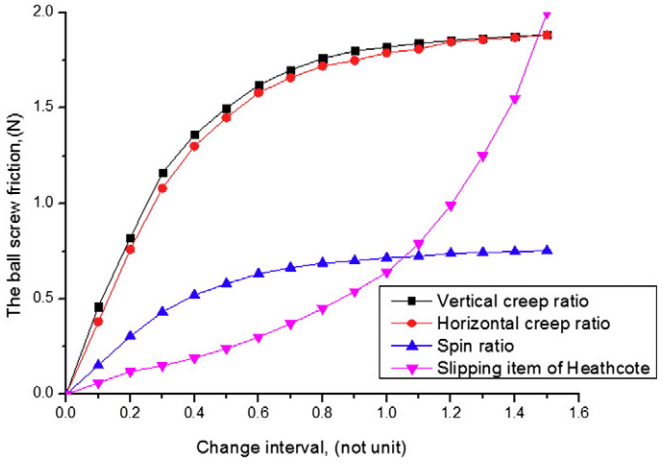

Fig. 9. The influence of creep parameters on ball screw friction between the ball and nut.

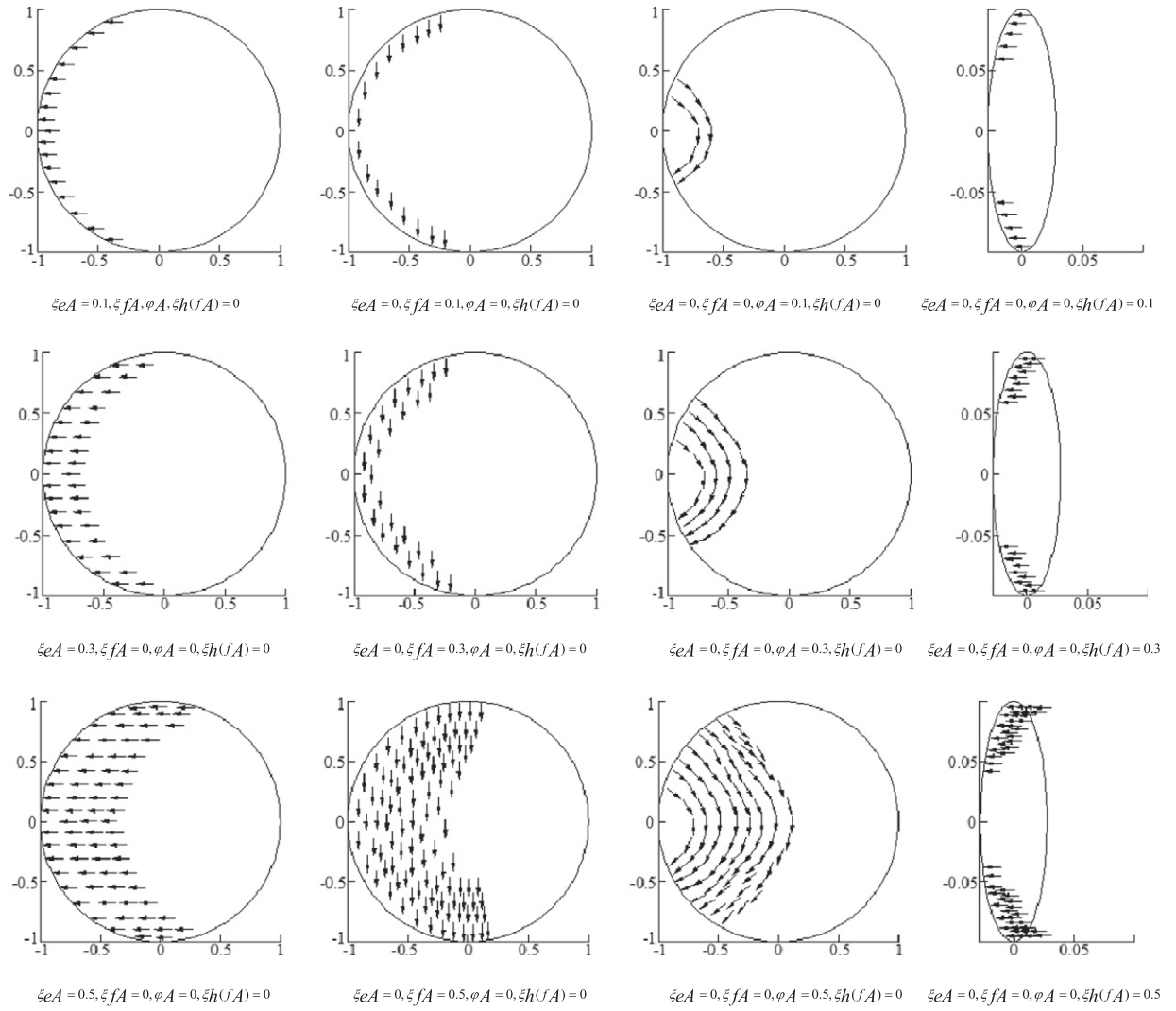

Fig. 10. The influence of creep parameters on friction distribution of the contact area between the ball and nut.

4. Conclusions

1. The friction model based on the creep analysis has been proven to be reasonable and effective, this provides a new perspective and approach that can be used to study ball screw friction.
2. Due to the nonlinear relationship between creep parameters and friction, it can be concluded that the basic parameters, which contains the creep parameters, such as the contact angle, ball diameter, preload and etc., have a nonlinear relationship with the friction of ball screw. At the same time, it is worth noting that the spin ratio can create friction perpendicular to the rolling direction independent of other parameters. This phenomenon proves that ignoring the effect of the spin ratio on the friction in a ball screw in the previous studies is unreasonable.
3. With an increase of slipping item of Heathcote, the influence of it on the ball screw friction will become more apparent, this means that the slipping item of Heathcote will become the main influencing factor on friction as the speed of the ball screw rotation increases.
4. The present study provides an intuitive way to understand the influence of creep parameters on ball screw friction and indicates the limitations of the Coulomb friction model.

Acknowledgments

The authors would like to thank the National Science and Technology Major Project of the Ministry of Science and Technology of China (2013ZX04008011) for the continuous funding support.

References

[1] C.-C. Wei, R.-S. Lai, Kinematical analyses and transmission efficiency of a preloaded ball screw operating at high rotational speeds, Mech. Mach. Theory 46 (2011) 880–898.
[2] S.G. Mu, X.Y. Feng, Study of the dynamic characteristic of high-speed ball screw, J. Human Univ. (Nat. Sci.) 38 (2011) 26–29.
[3] A.B. Jones, A general theory for elastically constrained ball and radial roller bearings under arbitrary load and velocity conditions, ASME J. Basic Eng. 12 (2) (1960) 309–320.
[4] T.A. Harris, Rolling bearing analysis, 2nd ed. Wiley, New York, 1984. 22–35.
[5] C.C. Wei, J.F. Lin, Kinematic analysis of the ball screw mechanism considering variable contact angles and elastic deformations, J. Mech. Des. 125 (2003) 717–733.
[6] D. Olaru, G.C. Puiu, L.C. Balan, et al., A new model to estimate friction torque in a ball screw system [M], Product Engineering, Springer, Netherlands, 2005. 333–346.
[7] A. Kamalzadeh, Precision control of high speed ball screw drives [D], Department of Mechanical Engineering, University of Waterloo, Waterloo, Canada, 2008. 86–99.
[8] Y.D. Su, Analysis and research study for the friction of a ball screw [D], School of mechanical Engineering of National Chung Hsing University, Taiwan, 2009. 43–54.
[9] J.J. Kalker, The analysis of the motion of the balls in an unlubricated angular contact thrust ball bearing [J], Wear 12 (l) (1968) 3–16.
[10] J.J. Kalker, The Influence of circulation of the balls in unlubricated angular-contact thrust ball bearing [J], Wear 13 (4) (1969) 293–300.
[11] J.J. Kalker, A fast algorithm for the simplified theory of rolling contact [J], Veh. Syst. Dyn. 11 (1) (1982) 1–13.
[12] J.J. Kalker, Three-Dimensional Elastic Bodies in Rolling contact [M], Kluwer Academic Publishers, Dordrecht, 1990. 32–45.
[13] L.I.N. MING-CHING, Design and mechanics of the ball screw mechanism [D], Mechanical Engineering of University of Wisconsin-Madison, USA, 1989. 23–26.
[14] Nanjing Technology Company, Nanjing ball screws technical information [M], The research of ball screw, China, 2012. 132–133.